INDUSTRIAL TOPCON SOLAR CELLS REALIZED BY A PECVD TUBE PROCESS

Frank Feldmann[1], Bernd Steinhauser[1], Thomas Pernau[2], Henning Nagel[1], Tobias Fellmeth[1], Sebastian Mack[1], Daniel Ourinson[1], Elmar Lohmüller[1], Jana Polzin[1,3], Ana Moldovan[1], Martin Bivour[1], Florian Clement[1], Jochen Rentsch[1], Martin Hermle[1], Stefan W. Glunz[1,3]

[1]Fraunhofer Institute for Solar Energy Systems ISE, Heidenhofstraße 2, 79110 Freiburg, Germany
[2]centrotherm international AG, Blaubeuren, Germany
[3]INATECH, University of Freiburg, Emmy-Noether-Straße 2, 79110 Freiburg, Germany
Phone: +49 761 - 4588 5287; e-mail: frank.feldmann@ise.fraunhofer.de

ABSTRACT: These days low-pressure chemical vapor deposition (LPCVD) is commonly used by the photovoltaic industry to deposit Si layers for tunnel oxide passivated contact (TOPCon). This work summarizes the development of an alternative TOPCon deposition process using a tube plasma-enhanced chemical vapor deposition (PECVD) tool. In the first part, the main results of the German federal project "Upgrade Si-PV" are summarized. The goal of this project was the transfer of the TOPCon process to an industrial-proven tube PECVD system. In the second part, recent progress on the implementation of this process into a TOPCon cell is presented. It is demonstrated that the PECVD system is capable of producing screen-printing compatible TOPCon layers yielding recombination currents of ≈ 3 fA/cm² and ≈ 200 fA/cm² in the passivated and metallized region, respectively. The best TOPCon cell which was realized with the PECVD process yielded the following current-voltage parameters: $V_{oc} = 700$ mV, $FF = 79.6\%$, $J_{sc} = 41.2$ mA/cm², and $\eta = 22.95\%$.
Keywords: PECVD, passivation, TOPCon, solar cell, silicon

1 INTRODUCTION

Poly-Si-based passivating contacts (herein referred to as TOPCon [1]) have enabled laboratory solar cells to surpass the 26% efficiency threshold [2, 3]. To date, research institutes and manufacturers are working towards the implementation of TOPCon into a lean and industrial-viable process flow. Most work has been dedicated to realizing the so-called industrial TOPCon (i-TOPCon) solar cell featuring a boron-diffused emitter, a TOPCon rear contact, and screen-printed contacts on both sides. Although the efficiency has climbed from 20.7% [4] through the lower 23% range [5, 6] to a record efficiency of 24.58% [7], there are still a few hurdles to overcome to convince the majority of cell makers to migrate from PERC to i-TOPCon. Especially the rather complex process flow, which typically requires additional high-temperature processes (BBr$_3$ diffusion for the emitter and POCl$_3$ diffusion to dope the intrinsic poly-Si layer), wet-chemistry (single-side etching of poly-Si at the front) as well as the use of silver-containing pastes at front and back increase the all-in cell costs compared to a PERC cell [8]. One step into the direction of a lean process flow is the replacement of the LPCVD technology by a deposition technology exhibiting higher throughput and uptime, capability of *in-situ* doping, and preferably single-sided deposition.

This manuscript is divided into two parts. Firstly, the main results of the federal project "Upgrade Technologies for Silicon Photovoltaics (Upgrade Si-PV)" which received funding from the German Ministry of Economic Affairs and Energy research [9] is summarized. Secondly, recent progress on the i-TOPCon cell featuring PECVD TOPCon is presented.

2 SUMMARY OF PROJECT UPGRADE SI-PV

The project "Upgrade Si-PV" was dedicated to promote understanding of the regeneration process for PERC solar cells (please see [10]) as well as advancing the industrialization of the TOPCon deposition technology by using a tube PECVD system of the company centrotherm.

2.1 Tunnel oxide

One work package was focussing on the investigation of alternative methods to form the tunnel oxide. To this end, the work on ozone-based (O$_3$) oxides published in [11] was continued and, additionally, a thermal tunnel oxide (referred to as TO) process was developed.
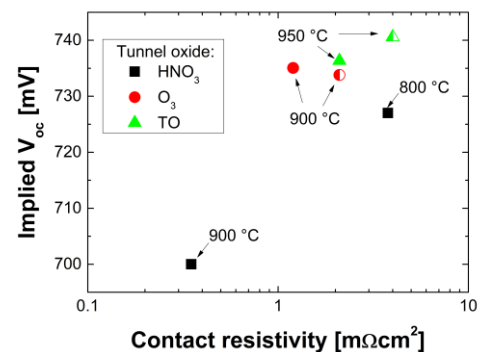

Figure 1: iV_{oc} plotted over contact resistivity measured on n-type 5 Ωcm FZ-Si wafers passivated by *n*-TOPCon featuring different tunnel oxides. The open symbols refer to TOPCon with a slightly reduced dopant concentration. The annealing temperatures are placed adjacently.

Fig. 1 shows the implied open-circuit voltage iV_{oc} vs. contact resistivity ρ_c measured by the transfer line method (TLM) of *n*-TOPCon featuring different tunnel oxides. Both, the O$_3$ oxide and TO show a superior surface passivation quality and a higher thermal stability compared to the nitric acid (HNO$_3$) oxide. The latter can be explained by the fact that both O$_3$ oxide and TO block phosphorus atoms diffusing from the poly-Si into the c-Si more effectively and presumably are less susceptible to balling-up of the oxide layer. Such distinctive behavior of different tunnel oxides upon annealing has recently been associated with the oxide's stoichiometry and thickness

[12]. Since TOPCon featuring the TO suppressed recombination most effectively and enabled reasonably low contact resistivity values of ≈ 2 mΩcm², this oxide became the standard process.

The interaction between tunnel oxide and dopant diffusion has been studied in more detail by using plasma grown and plasma nitrided tunnel oxides [13]. The doping profiles which are depicted in Fig. 2 were recorded by time-of-flight secondary ion mass spectroscopy (ToF-SIMS) and phosphorus was found to pile up at the poly-Si/SiO$_x$ interface while boron readily diffused through the oxide thereby forming a less shallow junction which adversely affects surface passivation. By using a nitrided oxide boron diffusion was suppressed successfully but a degradation of surface passivation quality was observed as well. Moreover, 1D and 3D numerical process simulation describing the diffusion profiles revealed that boron diffusion through pinholes contributes little to the aggregate diffusion profile in the c-Si which is accessible via electrochemical capacitance-voltage profiling.
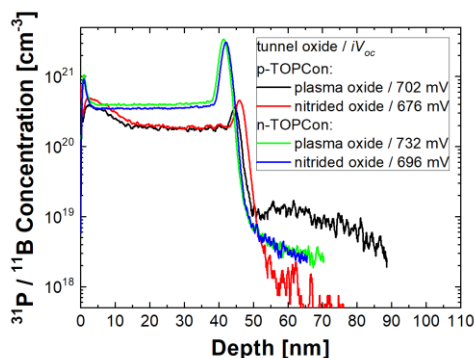

Figure 2: ToF-SIMS profiles of n-type and p-type TOPCon structures featuring a plasma oxide and a plasma nitrided oxide, respectively. The iV_{oc} values provided in the graph's legend were determined after furnace anneal and hydrogenation.

2.2 Development of PECVD tube process

The main objective of the given project was the transfer of the TOPCon deposition process from the laboratory PECVD tool Roth&Rau AK-400M to the industrial PECVD tool centrotherm cPLASMA 2000. The main development was performed using a horizontal boat configuration as displayed in Fig. 3. Following up on the first encouraging results that were published in [14], a process was developed that is characterized as follows:

- *In-situ* doping via addition of phosphine (PH$_3$)
- High deposition rate of ≈ 12 nm/min
- Low H-content in layers permits growth of films thicker than 200 nm
- Excellent surface passivation quality ($J_0 \leq 1$ fA/cm² on planar and $J_0 \approx 3$ fA/cm² on textured surfaces)
- Homogeneous deposition and passivation quality over the whole boat (see Fig. 3)

As reported in [15], the deposition process was successfully transferred to a vertical boat which resembles a boat configuration used in production.
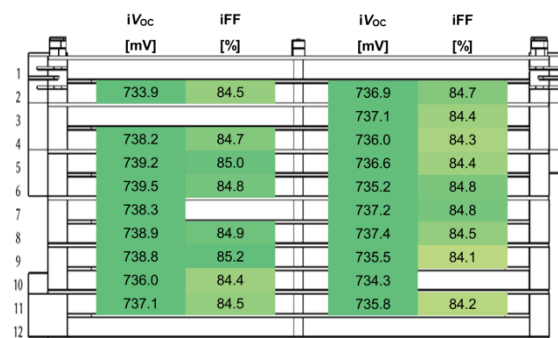

Figure 3: (Top) A photograph of a horizontal PECVD boat. (Bottom) A side view schematic of the horizontal boat displaying the iV_{oc} and iFF values determined by QSSPC on the respective wafers.

2.3 Hydrogenation of TOPCon

The saturation of dangling bonds at the Si/SiO$_x$ interface [16] and presumably the elimination of defects within the poly-Si layer [17] via hydrogen is a key process step enabling record-high surface passivation quality. At Fraunhofer ISE, a process called remote plasma hydrogen passivation (RPHP) [18] soon became the standard hydrogenation process for small wafer sizes. In the third work package alternative hydrogenation processes were investigated.

One important finding was that processes which solely supply molecular hydrogen are less effective than processes based on atomic hydrogen [19] (see also [20]). The latter can be released from atomic layer deposited (ALD) Al$_2$O$_3$:H, PECVD SiN$_x$:H, and even hydrogen-containing transparent conductive oxide (TCO) layers [21] during a low-temperature anneal at about 400°C or a fast-firing process. The process sequence PECVD SiN$_x$ and firing was studied in more detail within the framework of the project "PV-BAT400". As presented at the 36th EU-PVSEC [15], SiN$_x$ layers with a higher refractive index (and thus more Si-H bonds) enable a superior passivation quality after firing compared to SiN$_x$ layers with a refractive index of less than 2.0. Using an optimized process sequence, J_0 values of about 3 fA/cm² can be achieved on rough surfaces. More details can be found in [22].

2.4 Free carrier absorption

In contrast to our 25.8%-efficient lab-type TOPCon cell, industrial TOPCon cells make use of thicker (150-200 nm) heavily-doped poly-Si layers which adversely affect the infrared response of silicon solar cells via free

carrier absorption (FCA). The influence of poly-Si doping level was studied experimentally on lab-type solar cells featuring a 140 nm thick poly-Si layer at the rear. Fig. 4 plots the J_{sc} losses attributed to FCA over poly-Si dopant concentration. The J_{sc} losses were calculated from the cells' external quantum efficiency (EQE) data in the infrared region. For more information, the reader is kindly referred to [23]. The dashed and dotted lines refer to FCA-induced J_{sc} losses obtained from numerical device simulation using the parameterization for FCA in c-Si which was determined by Baker-Finch et al. [24]. It can be seen that FCA losses increased significantly with dopant concentration and that numerical device simulation using the mean value or upper limit of the FCA parameterization can reproduce the experimentally obtained data points. From this graph, it is obvious that thick poly-Si layers with $N_{D,poly-Si} \geq 1.5 \times 10^{20}$ cm^{-3} lead to significant FCA losses and, therefore, should be avoided.
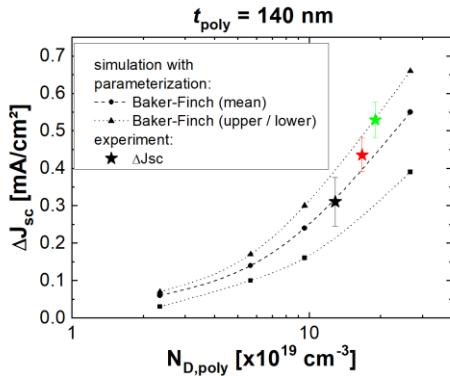

Figure 4: J_{sc} losses caused by FCA are plotted over poly-Si doping concentration. Stars refer to experimentally obtained data points and dashed and dotted lines label results from numerical simulation.

2.5 TOPCon Cells with an area of 10x10 cm²

Within the project "Upgrade Si-PV" 10x10 cm² solar cells were processed using 250 µm thick n-type 1 Ωcm FZ-Si wafers and the results were published in [25]. The solar cells featured a homogeneous boron emitter with an emitter sheet resistance $R_{sh} = 140$ Ω/sq and a TOPCon rear contact with full-area physical vapor deposited (PVD) silver metallization. A three busbar H-pattern layout was realized at the front employing either one of the two following process sequences:

  i)   Photolithography (PL) and PVD metallization with a metallized area fraction of ≈ 0.5% (non-contacting busbars)
  ii) laser contact opening (LCO) and plating of NiCuAg with a metallized area fraction (A_{met}) of ≈ 1.5% (contacting busbars)

The current-voltage (I-V) parameters of the best cells are shown in Table I. The cell featuring PVD metallization achieved a high V_{oc} of 713 mV which is very close to the maximum V_{oc} measured internally on cells featuring a homogeneous emitter. Significantly higher V_{oc} values can only be obtained by introducing a selective emitter scheme or TOPCon underneath the front metallization. On the other hand, the cells with plated metallization showed a lower V_{oc} of 697 mV due to enlarged A_{met} and thus increased contact recombination. The latter can be attributed to laser-induced damage of the emitter bulk in the near-surface region which was not cured by a high-temperature process such as firing. Nevertheless, these results indicate, that the V_{oc} of a TOPCon cell will be limited by recombination at the front surface in most cases.

Table I: I-V parameters of best 10x10 cm² solar cells independently confirmed by Fraunhofer ISE CalLab PVCells.

Front metallization	V_{OC}	J_{SC}	FF	pFF	η
	[mV]	[mA/cm²]	[%]	[%]	[%]
PL + PVD	713	41.4	83.1	84.8	**24.5**
LCO + Plating	697	41.4	81.2	84.3	**23.4**

3 RECENT TOPCON SOLAR CELLS

3.1 Experimental Details

Industrial TOPCon solar cells were realized on M2-sized n-type 1 Ωcm Cz-Si wafers which were supplied by LONGi. The process sequence is depicted in Fig. 5. After saw damage removal, texturing, and cleaning, three different boron emitters were realized by atmospheric pressure BBr$_3$ diffusion. The boron emitters are characterized as follows:

  -   1) $R_{sh} \approx 110$ Ω/sq, $J_{0e} \approx 27$ fA/cm²
  -   2) $R_{sh} \approx 120$ Ω/sq, $J_{0e} \approx 22$ fA/cm²
  -   3) $R_{sh} \approx 150$ Ω/sq, $J_{0e} \approx 15$ fA/cm²

More information on the processes can be found in [26]. After wet-chemical edge isolation, a tunnel oxide layer was grown thermally and 150 nm in-situ phosphorus-doped a-Si was deposited by a centrotherm cPLASMA PECVD tool. Since the deposition process produces a minimal wrap around at the edges, a wet-chemical process was employed to remove the a-Si layer from the front surface. Thereafter, TOPCon was activated by a furnace anneal. The front surface was passivated by a stack of ALD Al$_2$O$_3$ and PECVD SiN$_x$:H. The rear received a SiN$_x$:H layer with a slightly higher refractive index – as outlined above. A busbarless grid design was applied by screen-printing a silver-aluminum (AgAl) paste on the front and a silver (Ag) paste on the rear side. The cells were fired in an industrial conveyor belt furnace at peak set temperatures ranging from 800°C to 840°C. The cells were measured using a Halm inline flash tester which is equipped with a Pasan PCB-Touch unit featuring a black, non-conductive chuck.
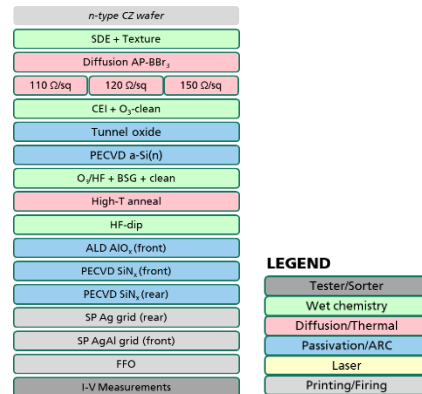

Figure 5: Process sequence of i-TOPCon cells featuring a tube PECVD process.

3.2 Interplay between TOPCon and metallization

The contact properties (i.e. $J_{0,met}$, ρ_c) of screen-printed fire-through contacts were studied on 100-200 nm thick TOPCon layers. Fig. 6 plots the J_{0met} values over nominal poly-Si thickness in dependence of firing temperature. The blue data points refer to data from literature [27, 28]. The results suggest that a poly-Si thickness of 100 nm or less is still critical for screen-printed and fired contacts as J_{0met} values above 1000 fA/cm² were determined from photoluminescence (PL) images. On the other hand, reasonably low J_{0met} values of about 200 fA/cm² were achieved on both 150 nm and 200 nm thick poly-Si contacts. In addition, low contact resistivity values of ≈ 1 mΩcm² were obtained for the metal/poly-Si interface.

For comparison with the solar cell's front side it is interesting to note that investigations on test structures featuring a boron-diffused emitter (not shown here) yielded $J_{0,met}$ values in the range of 1000-2000 fA/cm² and showed that contact resistivity decreased from 10 mΩcm² down to 2-3 mΩcm² with increasing temperature.
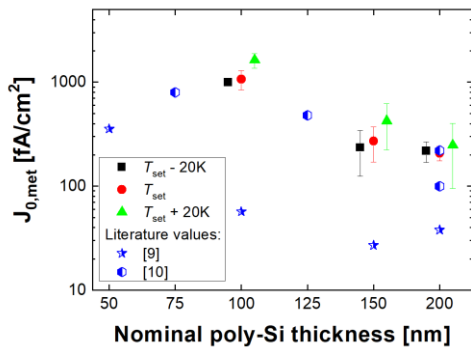

Figure 6: $J_{0,met}$ values plotted over nominal poly-Si thickness for three different set peak firing temperatures T_{set}. Please note that some data points are adjacently placed for clarity.
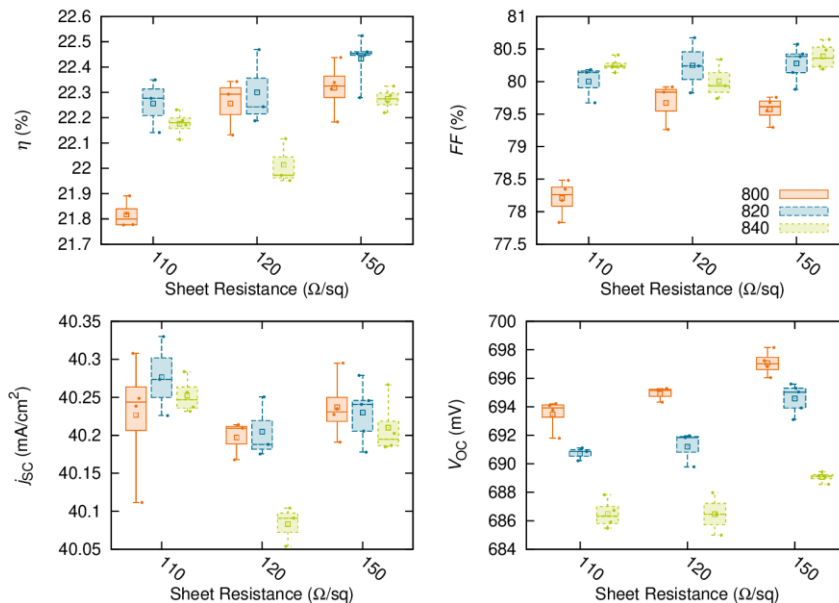
3.3 Solar cells

Fig. 7 plots the light *I-V* parameters of the TOPCon solar cells over the emitter sheet resistance. The differently colored boxes refer to different set peak firing temperatures. One can see that the firing temperature had a strong impact on both the cells' V_{oc} and *FF*. V_{oc} decreased with increasing firing temperature by about 10 mV. Such loss can mainly be ascribed to an increased recombination rate at the front metal contacts. The application of an emitter with a higher R_{sh} yielded a slight increase in V_{oc} from 694 mV ($R_{sh} = 110$ Ω/sq) to 698 mV ($R_{sh} = 150$ Ω/sq). Compared to the V_{oc}, the *FF* shows a quite different dependence on firing temperature. At the lowest firing temperature of 800°C, the lowest *FF* values were measured within each group. In case of the emitter exhibiting $R_{sh} = 110$ Ω/sq, a mean *FF* of 78.2% was obtained. The cells of this group which were fired at 820°C and 840°C, respectively, yielded substantially higher *FF* values above 80.0%. The groups featuring more resistive emitters exhibited similar *FF* values in the range of 80.0% to 80.7% for both firing temperatures 820°C and 840°C. The increase in *FF* with firing temperate went along with a reduction in series resistance from ≈ 0.8 Ωcm² ($R_{sh} = 110$ Ω/sq / 800°C) to ≈ 0.45 Ωcm² ($R_{sh} = 110$ Ω/sq / 840°C). This effect can be explained by improved contact formation at the front. The cells' J_{sc} averaged to 40.2 mA/cm² and did not show any significant dependence on emitter process or firing temperature.

The most efficient cell was then coated with magnesium fluoride (MgF$_2$) to further reduce reflection losses and has been measured by Fraunhofer ISE CalLab PVCells using a reflective chuck and 30 wires. The independently confirmed light *I-V* parameters are displayed in Table II and an efficiency of close to 23% was obtained.

Figure 7: Light *I-V* parameters of TOPCon solar cells as a function of emitter sheet resistance.

Table II: The *I-V* parameters of the champion solar cell were independently confirmed by Fraunhofer ISE CalLab PVCells. The solar cell was measured on a reflective chuck using 30 wires.

	V_{OC} [mV]	J_{SC} [mA/cm^2]	*FF* [%]	η [%]
Champion	700	41.2	79.6	22.95

4 SUMMARY AND OUTLOOK

The work within the project "Upgrade Si-PV" laid the foundations for advancing the industrialization of centrotherm's cPLASMA tube PECVD system. The TOPCon PECVD process is characterized by the following key features:
- Excellent surface passivation quality ($J_0 \leq 1$ fA/cm² on planar and $J_0 \approx 3$ fA/cm² on rough surfaces)
- In-situ doping via addition of PH_3
- High deposition rate of ≈ 12 nm/min
- Layers are compatible with screen-printed metallization

These layers were then successfully integrated into TOPCon solar cells achieving an independently confirmed efficiency of 22.95% and a V_{oc} of 700 mV.

Our results show that the limiting factor of our cell is the recombination at the interface between metal and homogeneous boron emitter. Hence, a more advanced emitter structure is the key to achieve higher efficiencies.

5 ACKNOWLEDGEMENTS

6 REFERENCES

[1] F. Feldmann, M. Bivour, C. Reichel, M. Hermle, and S. W. Glunz, "Passivated rear contacts for high-efficiency n-type Si solar cells providing high interface passivation quality and excellent transport characteristics," *Sol Energ Mat Sol C*, vol. 120, Part A, pp. 270–274, 2014, doi: 10.1016/j.solmat.2013.09.017.

[2] M. A. Green *et al.,* "Solar cell efficiency tables (Version 53)," *Prog Photovolt Res Appl*, vol. 27, no. 1, pp. 3–12, 2019, doi: 10.1002/pip.3102.

[3] F. Haase *et al.,* "Laser contact openings for local poly-Si-metal contacts enabling 26.1%-efficient POLO-IBC solar cells," *Sol. Energy Mater. Sol. Cells*, vol. 186, pp. 184–193, 2018, doi: 10.1016/j.solmat.2018.06.020.

[4] M. K. Stodolny *et al.,* "n-Type polysilicon passivating contact for industrial bifacial n-type solar cells," *Sol Energ Mat Sol C*, doi: 10.1016/j.solmat.2016.06.034.

[5] Y. Chen *et al.,* "Mass production of industrial tunnel oxide passivated contacts (i-TOPCon) silicon solar cells with average efficiency over 23% and modules over 345 W," *Progress in Photovoltaics: Research and Applications*, vol. 41, p. 46, 2019, doi: 10.1002/pip.3180.

[6] N. Nandakumar *et al.,* "Investigation of 23% monoPoly Screen-Printed Silicon Solar Cells with an Industrial Rear Passivated Contact," in *2019 IEEE 46th Photovoltaic Specialists Conference (PVSC)*, Chicago, IL, USA, Jun. 2019 - Jun. 2019, pp. 1463–1465.

[7] D. Chen *et al.,* "24.58% total area efficiency of screen-printed, large area industrial silicon solar cells with the tunnel oxide passivated contacts (i-TOPCon) design," *Sol. Energy Mater. Sol. Cells*, vol. 206, p. 110258, 2020, doi: 10.1016/j.solmat.2019.110258.

[8] B. Kafle, B. Goraya, Mack, Feldmann, Frank, Sebastian., S. Nold, and J. Rentsch, "TOPCon - Technology Options for Cost Efficient Industrial Manufacturing," in *Proceedings of the 37th European Photovoltaic Solar Energy Conference and Exhibition*, 2020.

[9] *EnArgus.* [Online]. Available: https:// www.enargus.de/pub/bscw.cgi/?op=enargus.eps2& q=%2201161126/1%22 (accessed: Feb. 5 2020).

[10] T. Pernau *et al.,* "Upgrade Technology for Silicon Photovoltaics - Part I: Industrial solution to minimize the negative impact of light induced degradation," in *Proceedings of the 37th European Photovoltaic Solar Energy Conference and Exhibition*, 2020.

[11] A. Moldovan, F. Feldmann, M. Zimmer, J. Rentsch, J. Benick, and M. Hermle, "Tunnel oxide passivated carrier-selective contacts based on ultra-thin SiO_2 layers," *Sol Energ Mat Sol C*, vol. 142, pp. 123–127, 2015, doi: 10.1016/j.solmat.2015.06.048.

[12] J.-I. Polzin *et al.,* "Temperature-induced stoichiometric changes in thermally grown interfacial oxide in tunnel-oxide passivating contacts," *Sol Energ Mat Sol C*, vol. 218, p. 110713, 2020, doi: 10.1016/j.solmat.2020.110713.

[13] F. Feldmann, J. Schön, J. Niess, W. Lerch, and M. Hermle, "Studying dopant diffusion from Poly-Si passivating contacts," *Sol Energ Mat Sol C*, vol. 200, p. 109978, 2019, doi: 10.1016/j.solmat.2019.109978.

[14] B. Steinhauser, J.-I. Polzin, F. Feldmann, M. Hermle, and S. W. Glunz, "Excellent Surface Passivation Quality on Crystalline Silicon Using Industrial-Scale Direct-Plasma TOPCon Deposition Technology," *Sol. RRL*, vol. 2, no. 7, p. 1800068, 2018, doi: 10.1002/solr.201800068.

[15] F. Feldmann *et al.,* "Large Area TOPCon Cells Realized by a PECVD Tube Process," 2019, doi: 10.4229/EUPVSEC20192019-2EO.1.4.

[16] M. Schnabel *et al.,* "Hydrogen passivation of poly-Si/SiO x contacts for Si solar cells using Al_2O_3 studied with deuterium," *Appl. Phys. Lett.*, vol. 112, no. 20, p. 203901, 2018, doi: 10.1063/1.5031118.

[17] T. N. Truong *et al.,* "Hydrogenation of Phosphorus-Doped Polycrystalline Silicon Films for Passivating Contact Solar Cells," *ACS applied*

materials & interfaces, vol. 11, no. 5, pp. 5554–5560, 2019, doi: 10.1021/acsami.8b19989.

[18] S. Lindekugel, H. Lautenschlager, T. Ruof, and S. Reber, "Plasma Hydrogen Passivation for Crystalline Silicon Thin-Films," 2008, doi: 10.4229/23RDEUPVSEC2008-3AV.1.15.

[19] J.-I. Polzin, F. Feldmann, B. Steinhauser, M. Hermle, and S. W. Glunz, "Study on the interfacial oxide in passivating contacts," in *15th International Conference on Concentrator Photovoltaic Systems (CPV-15)*, Fes, Morocco, 2019, p. 40016.

[20] J. Schmidt, R. Peibst, and R. Brendel, "Surface passivation of crystalline silicon solar cells: Present and future," *Sol. Energy Mater. Sol. Cells*, vol. 187, pp. 39–54, 2018, doi: 10.1016/j.solmat.2018.06.047.

[21] L. Tutsch *et al.,* "Implementing transparent conducting oxides by DC sputtering on ultrathin SiOx / poly-Si passivating contacts," *Sol. Energy Mater. Sol. Cells*, vol. 200, p. 109960, 2019, doi: 10.1016/j.solmat.2019.109960.

[22] B. Steinhauser, F. Feldmann, D. Ourinson, H. Nagel, T. Fellmeth, and M. Hermle, "On the Influence of the SiNx Composition on the Firing Stability of Poly-Si/SiNx Stacks," *phys. status solidi a*, 2020, doi: 10.1002/pssa.202000333.

[23] F. Feldmann, M. Nicolai, R. Müller, C. Reichel, and M. Hermle, "Optical and electrical characterization of poly-Si/SiO x contacts and their implications on solar cell design," *Energy Procedia*, vol. 124, pp. 31–37, 2017, doi: 10.1016/j.egypro.2017.09.336.

[24] S. C. Baker-Finch, K. R. McIntosh, Di Yan, K. C. Fong, and T. C. Kho, "Near-infrared free carrier absorption in heavily doped silicon," *Journal of Applied Physics*, vol. 116, no. 6, p. 63106, 2014, doi: 10.1063/1.4893176.

[25] B. Steinhauser *et al.,* "Large Area TOPCon Technology Achieving 23.4% Efficiency," in *2018 IEEE 7th World Conference on Photovoltaic Energy Conversion (WCPEC) (A Joint Conference of 45th IEEE PVSC, 28th PVSEC & 34th EU PVSEC)*, Waikoloa Village, HI, Jun. 2018 - Jun. 2018, pp. 1507–1510.

[26] E. Lohmüller *et al.,* "BBr3 diffusion: process optimization for high-quality emitters with industrial cycle times," in *Proceedings of the 37th European Photovoltaic Solar Energy Conference and Exhibition*, 2020.

[27] P. Padhamnath *et al.,* "Development of thin polysilicon layers for application in monoPoly™ cells with screen-printed and fired metallization," *Sol. Energy Mater. Sol. Cells*, vol. 207, p. 110358, 2020, doi: 10.1016/j.solmat.2019.110358.

[28] H. E. Çiftpınar *et al.,* "Study of screen printed metallization for polysilicon based passivating contacts," *Energy Procedia*, vol. 124, pp. 851–861, 2017, doi: 10.1016/j.egypro.2017.09.242.